White Dwarfs:
Origin of Atmospheric Composition

Dave Nero

9/11/2007

Outline

- Background
- DA, Non-DA
- Non-DA Gap, DB Gap
- DB, DQ
- DO, DC, DZ
- 1000 Word Summary

http://www.upscalegallery.com

References - Background

- Sion, E. M., Greenstein, J. L., Landstreet, J. D., Liebert, J., Shipman, H. L., and Wegner, G. A. 1983, ApJ, 269, 253
  - "A PROPOSED NEW WHITE DWARF SPECTRAL CLASSIFICATION SYSTEM"
- Koester, D. and Chanmugam, G. 1990, Rep. Prog. Phys., 53, 837
  - "Physics of white dwarf stars"

References – DA, Non-DA

- Barstow, M. A., Fleming, T. A., Diamond, C. J., Finley, D. S., Sansom, A. E., Rosen, S. R., Koester, D., Marsh, M. C., Holberg, J. B., and Kidder, K. 1993, MNRAS, 264, 16
  - "ROSAT studies of the composition and structure of DA white dwarf atmospheres"
- Bergeron, P., Wesemael, F., Fontain, G., and Liebert, J. 1990, ApJ, 351, L21
  - "ON THE SURFACE COMPOSITION OF COOL, HYDROGEN-LINE WHITE DWARFS: DISCOVERY OF HELIUDOM IN THE ATMOSPHERES OF COOL DA STARS AND EVIDENCE FOR CONVECTIVE MIXING"

References – Non-DA Gap, DB Gap

- Malo, A., Wesemael, F., and Bergeron, P. 1999, ApJ, 517, 901
  - "PHYSICAL PROCESSES IN THE ATMOSPHERES OF COOL WHITE DWARFS AND THE NATURE OF THE NON-DA GAP"
- Shibahashi, H. 2006, Convection in Astrophysics, Proceedings IAU Sympsium No. 239
  - "The DB gap of white dwarfs and semiconvection"

References – DB, DQ

- Althaus, L.G., Serenelli, A. M., Panei, J. A., Corsico, A. H., Garcia-Berro, E., and Scoccola, C. G., 2005, A&A, 435, 631
  - "The formation and evolution of hydrogen-deficient post-AGB white dwarfs: The emerging chemical profile and the expectations for the PG 1159-DB-DQ evolutionary connection"
- Scoccola, C. G., Althaus, L.G., Serenelli, A. M., Rohrmann, R. D., and Corsico, A. H. 2006, A&A, 451, 147
  - "DQ white-dwarf stars with low C abundance: possible progenitors"

References – DO, DC, DZ

- Hugelmeyer, S. D., Dreizler, S., Werner, K., Krzesinski, J., Nitta, A., and Kleinman, S. J. 2005, A&A 442, 309
  - "Spectral analyses of DO white dwarfs and PG 1159 stars from the Sloan Digital Sky Survey"
- Harris, H. C., Dahn, C. C., Vrba, F. J., Henden, A. A., Liebert, J., Schmidt, G. D. and Reid, I. N. 1999, APJ, 524, 1000
  - "A VERY LOW LUMINOSITY, VERY COOL, DC WHITE DWARF"
- Koester, D., Wegner, G., and Kilkenny, D. 1990, ApJ, 350, 329
  - "MODEL ATMOSPHERE ANALYSIS OF THE DZ WHITE DWARF K789-37"

Spectral Classification System

- D for “degenerate”
- Uppercase letter for primary spectral feature

DEFINITION OF PRIMARY SYMBOLS: PRIMARY SPECTRAL

Spectral Type	Characteristics
DA	Only Balmer lines; no He I or metals present
DB	He I lines; no H or metals present
DC	Continuous spectrum, no lines deeper than 5% in any part of the electromagnetic spectrum
DO	He II strong: He I or H present
DZ	Metal lines only; no H or He
DQ	Carbon features, either atomic or molecular, in any part of the electromagnetic spectrum

Spectral Classification

- A second uppercase letter for secondary spectral features
- Additional symbols
  - P – polarized magnetic star
  - H – unpolarized magnetic star
  - X – peculiar or unclassifiable feature(s)
  - V – variable

Spectral Classification

- Temperature index
  - 0-9 given by 50400/T
- Examples:

EXAMPLES OF THE PROPOSED NEW CLASSIFICATION

Example	Old	New
1. A white dwarf with only H I lines; $T_e = 30{,}000$ K (e.g., EG 157)	DA	DA1
2. A white dwarf with only He I lines; $T_e = 15{,}000$ K (e.g., L1573−31)	DB	DB3
3. A white dwarf with no lines deeper than 5% in any part of the electromagnetic spectrum; $T_e = 8000$ K (e.g., EG 1)	DC	DC6
4. A DB Star with Ca II; $T_e = 14{,}000$ K (e.g., GD 40)	DBPEC	DBZ4
5. A polarized magnetic white dwarf with helium and hydrogen, but with helium dominant; $T_e = 20{,}000$ K (e.g., Feige 7)	DBAP	DBAP3
6. A cool white dwarf with Ca II, Fe I; $T_e = 6000$ K (e.g., vMa 2)............	DG	DZ8
7. A DA, F star; $T_e = 7400$ K (e.g., G74−7)	DA, F	DAZ7
8. A peculiar metallic line white dwarf with H; $T_e = 8500$ K (e.g., Ross 640)	DFPEC	DZA7
9. A DA star with weak He II (λ4686); $T_e = 50{,}000$ K (e.g., HZ 34)...........	DA	DZ01
10. A peculiar magnetic white dwarf; unidentified composition with no detectable polarization; $T_e = 25{,}000$ K (e.g., GD 229)	DXP	DXH3
11. A cool white dwarf showing C_2 bands in the optical and C I lines in the ultraviolet; $T_e = 8500$ K (e.g., L879−14)	C_2	DQ6
12. A DO white dwarf with N V (λ1240) $T_e = 70{,}000$ K	DO	DOZ1

Two Explanations for Observed Spectral Types

- WDs can change their atmospheric composition (i.e. spectral type) as they cool
  - “DB gap” and “non-DA gap”
- Different spectral types have different progenitors
  - Strong variation in He/H ratio in planetary nebulae

Physical Processes in the Non-Degenerate Envelope

- Diffusion
  - Heavier elements sink, lighter elements float
  - Timescale much shorter than evolutionary timescale
    - Should ONLY see H
- Meridional circulation
  - Caused by rapid rotation
  - May be non-negligible for hot WDs

Physical Processes in the Non-Degenerate Envelope

- Mass loss
  - Observed for hot DAs
  - BUT H layer is very thin and DA is most common type
- Accretion of interstellar matter
  - Too slow to affect hot DAs, but important for DZs

Physical Processes in the Non-Degenerate Envelope

- Radiative levitation
  - Absorption of radiation decreases effective gravity
  - Varies by species
- Convection
  - Probably important
  - Species completely mixed within convection zone

DA White Dwarfs

- Thin H layer over much thicker He layer
- Exist for a large range of T
  - Most with T>40,000K show traces of He
  - Those with T>50,000k also show traces of metals
  - Most with T<40,000K show little or no He
- Lower gravity stars show more non-H features
  - => Radiative Levitation

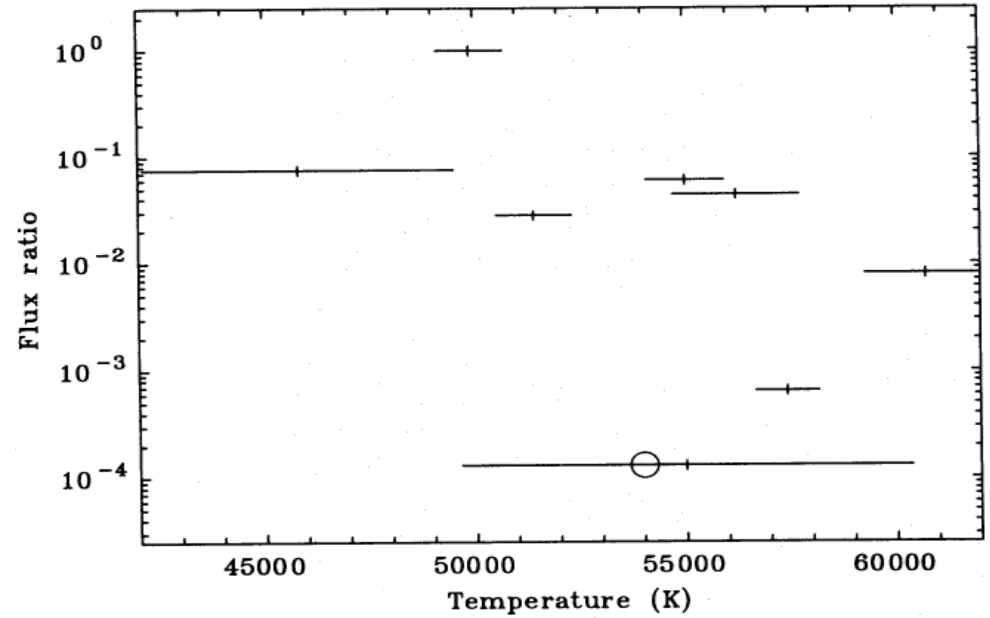

Figure 10. Ratio of the estimated emergent S1 fluxes to the values predicted for a pure H atmosphere as a function of temperature. The sample is restricted to those white dwarfs with temperatures above 50 000 K and low H I columns.

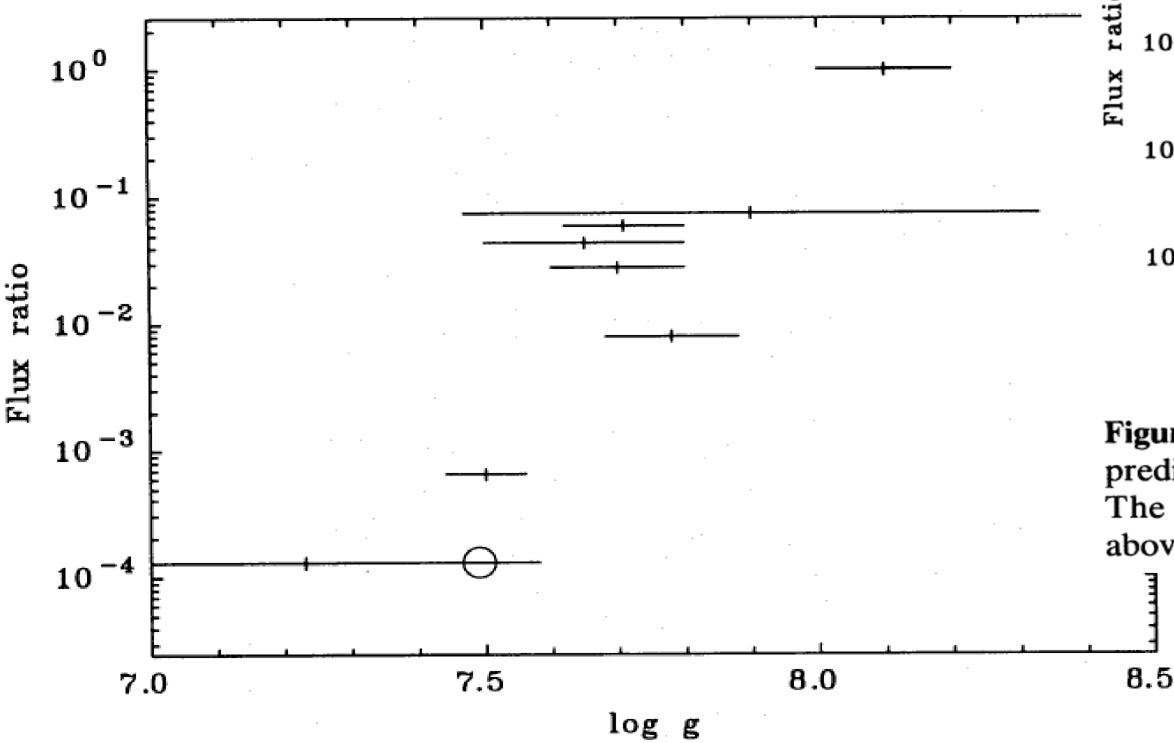

Figure 9. Ratio of the estimated emergent S1 fluxes to the values predicted for a pure H atmosphere as a function of log *g*. The sample is restricted to those white dwarfs with temperatures above 50 000 K and low H I columns.

Non-DA White Dwarfs

- The ratio of DA/non-DA varies strongly with T
  - Convection

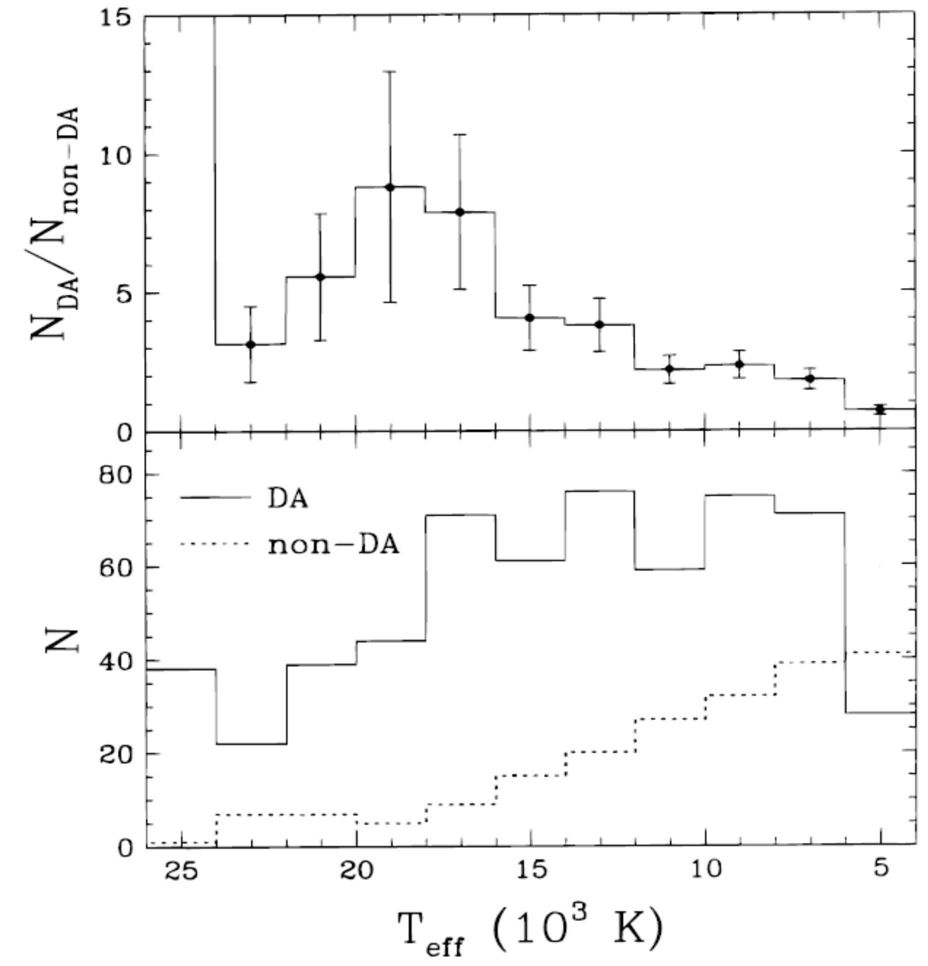

FIG. 1.—*Bottom*: Number of DA and non-DA stars in the McCook & Sion catalog, including new spectral types based on our own spectroscopic observations, as a function of effective temperature in 2000 K bins, the latter estimated from published color indices (see text). *Top*: DA to non-DA ratio as a function of T_{eff} for the same data set; error bars represent the Poisson statistics of each bin.

Bergeron et al. 1997, 108, 339

Non-DA White Dwarfs

- He lines not visible when T < 13,000K (even if He/H > 1)

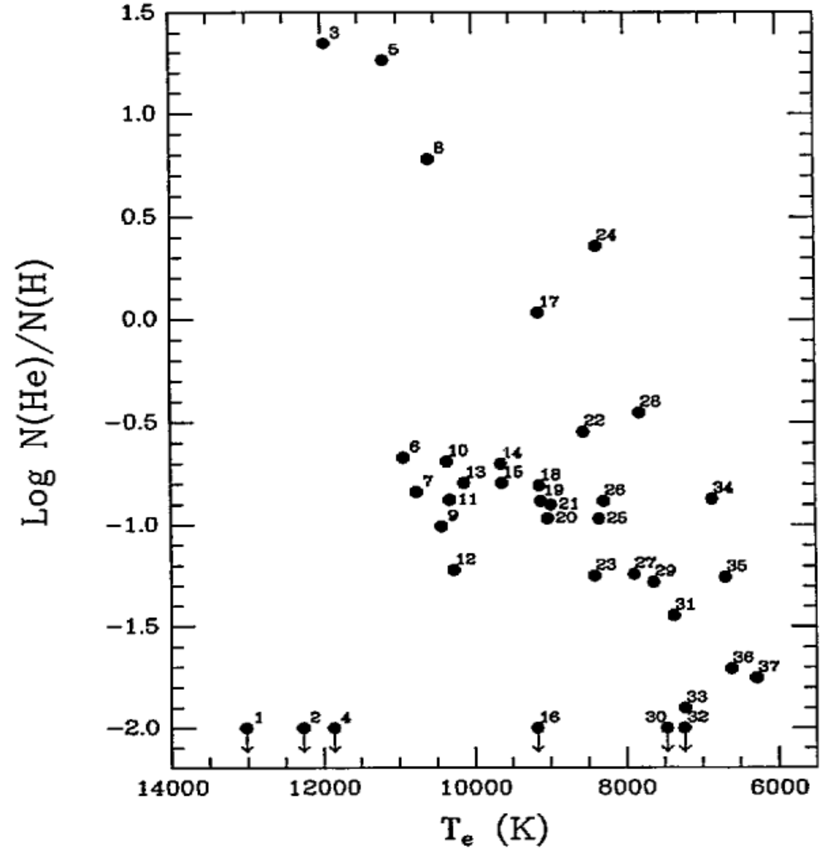

FIG. 1.—Helium abundances determined in cool DA white dwarfs as a function of effective temperature. The upper limits of $N(\mathrm{He})/N(\mathrm{H}) = 0.01$ are completely equivalent, from a spectroscopic point of view, with pure hydrogen atmospheres and represent the detection limit of our technique. The various stars are (1) GD 165, (2) G238–53, (3) G1–7, (4) GD 66, (5) G67–23, (6) GD 275, (7) PG 1149+057, (8) PG 1237−028, (9) G61–17, (10) GD 340, (11) G172–4, (12) GD 83, (13) G121–22, (14) GD 290, (15) L710-30, (16) L587-77A, (17) GD 25, (18), G115–9, (19) PG 0901+140, (20) G28–13, (21) G93–53, (22) G49–33, (23) G175–46, (24) G117–25, (25) G187–32, (26) G1–45, (27) G90–28, (28) G92–40, (29) GD 69, (30) GD 96, (31) R627, (32) G259–21, (33) G74–7, (34) G108–26, (35) G156–64, (36) G144–51, and (37) G217–37.

Non-DA Gap

- No non-DA stars between 5100K – 6100K
- Cooling sequence: non-DA -> DA -> non-DA
- Seems to be an opacity effect
  - Not well understood

DB Gap

- No DBs found with 30,000K < T < 45,000K
  - Have DOs at T>45,000k and DBs at T<30,000K
  - Cooling sequence: DO -> DA -> DB
- Possibly explained by convection:
  - At T>45,000K, have He II/III convection
  - At T<30,000K, have He I/II convection
  - No convection for 30,000K < T < 45,000K

DB White Dwarfs

- 11,000K < T < 30,000K
- Possible origin: “born-again” scenario (Fujimoto, 1977, PASJ, 29, 331)
  - Very late He-shell burning by WD remnant just before end of H burning
  - Thermal pulse engulfs and completely burns remaining H envelope
  - Leaves a hot post-AGB star -> DO -> DB
    - PG 1159

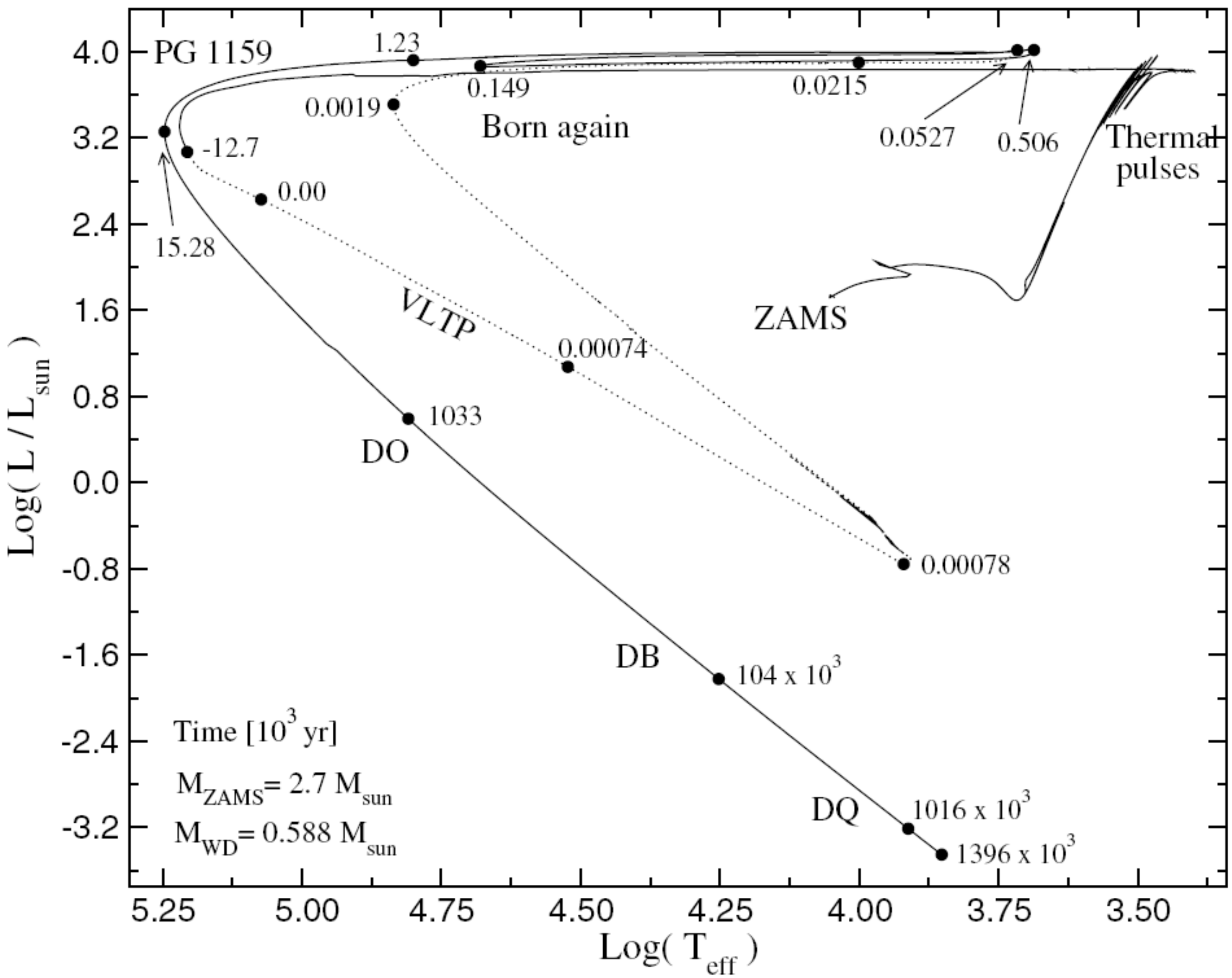

Fig. 1. Hertzsprung-Russell diagram for the complete evolution of our 2.7 $M_{\odot}$ stellar model from the ZAMS to the white dwarf domain. The star experiences a very last thermal pulse (VLTP) on its early cooling phase after hydrogen burning has almost ceased. The following evolutionary stages correspond to the born-again phase and are depicted, together with the VLTP stage with dotted lines. The numbers close to the filled dots along the evolutionary track correspond to the age (in 10^3 yr) counted from the occurrence of the peak of the last thermal pulse. The domain of the PG 1159, DO, DB and DQ stars are indicated, as well as the thermal pulse and born-again stages. As a result of mass loss episodes, the stellar mass decreases from 2.7 to 0.5885 $M_{\odot}$. After the born-again episode, the hydrogen-deficient post-AGB remnant experiences a second excursion towards lower temperatures before reaching eventually its terminal white dwarf track.

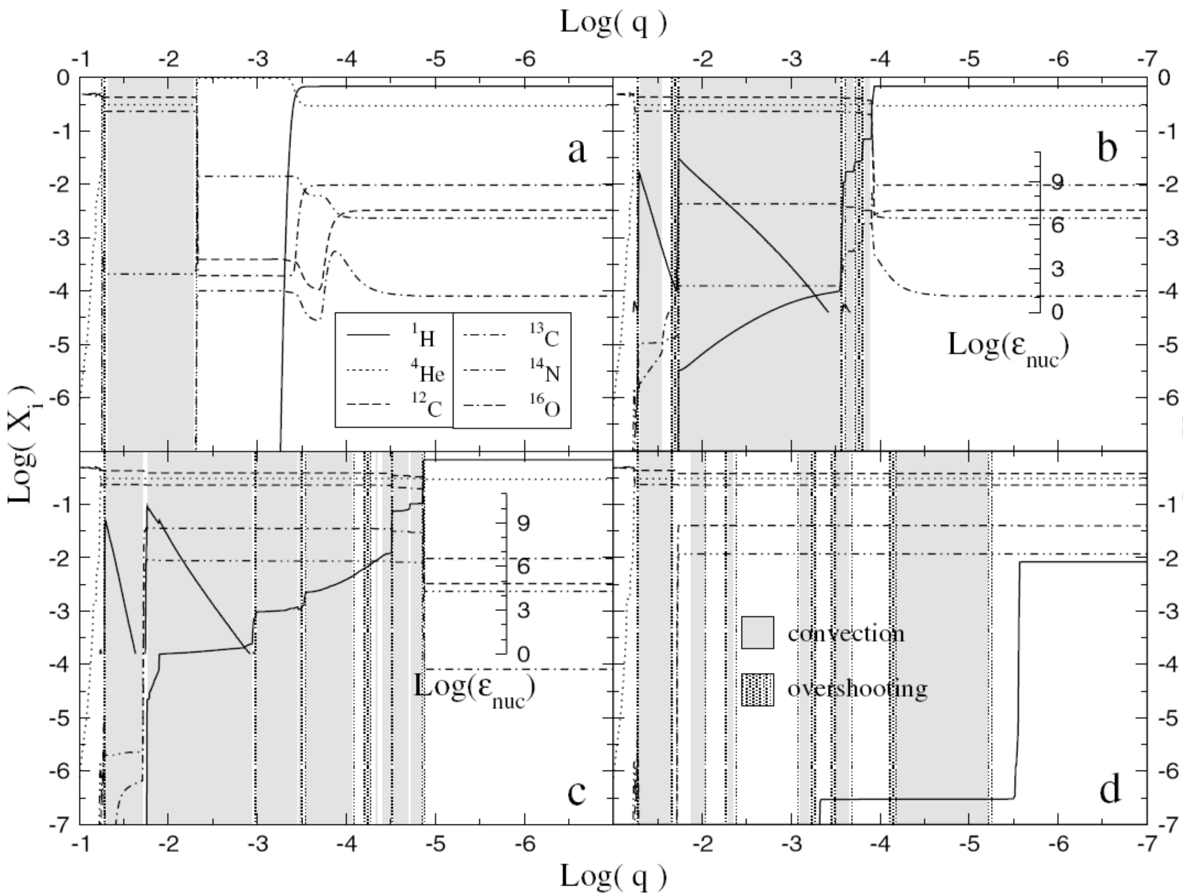

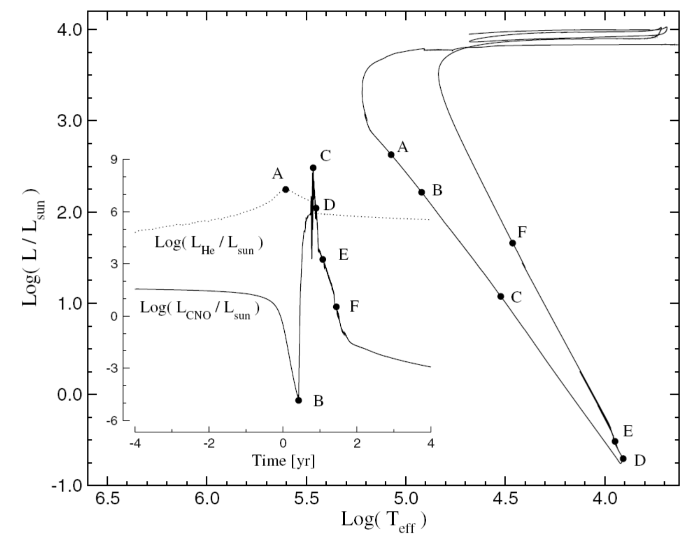

Fig. 5. Internal abundance distribution of ^{1}H, ^{4}He, ^{12}C, ^{13}C, ^{14}N and ^{16}O as a function of the outer mass fraction q for the 0.5885 $M_{\odot}$ remnant at various selected epochs during the course of the last helium thermal pulse. Panel **a)** corresponds to the moment just before the occurrence of the peak helium-burning luminosity (point A in Fig. 4). The situation when the outward-moving, helium-flash convection zone has reached the base of the hydrogen-rich envelope (between points B and C in Fig. 4) is illustrated by panel **b)**. Note that protons are ingested into deeper and hotter layers. As a result of the ongoing hydrogen burning a small radiative and salt-finger zone establishes at $\log q \approx -1.6$, which splits the convection zone into two. The situation two weeks later is visualized in panel **c)**. During this time, the convection zone powered by hydrogen burning propagates outwards. Finally, panel **d)** illustrates the abundance profiles near point F in Fig. 4. Only traces of hydrogen remain after hydrogen burning. Nuclear energy release due to hydrogen and helium burning are also shown in panel **b)** and **c)**.

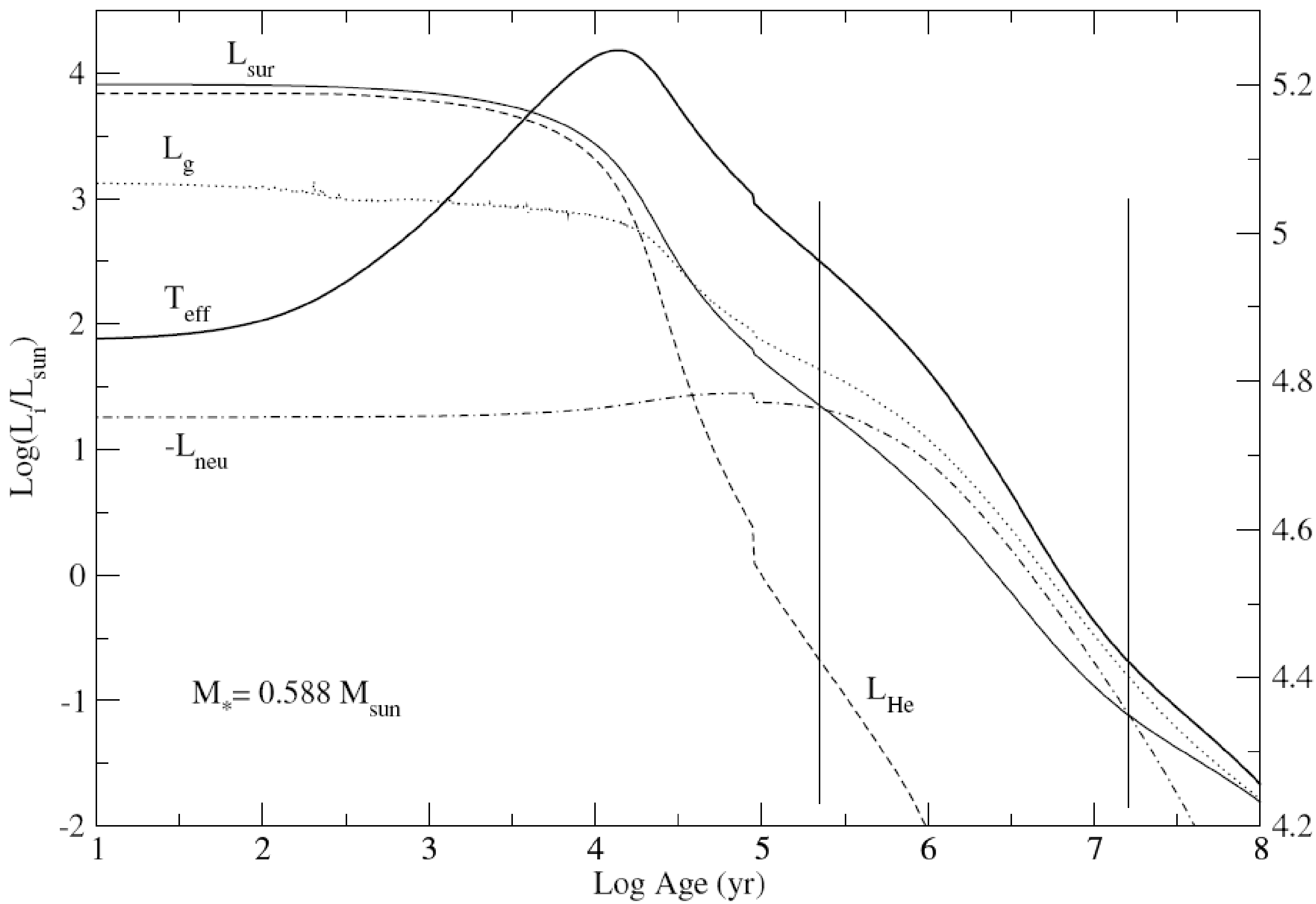

Fig. 7. Time-dependence of the different luminosity contributions (in solar units) for the post born again 0.5885 $M_{\odot}$ remnant of the evolution of the 2.7 $M_{\odot}$ star: surface luminosity, $L_{\rm sur}$, helium burning luminosity, $L_{\rm He}$, neutrino losses, $L_{\rm neu}$ and rate of gravothermal (compressional plus thermal) energy release $L_{\rm g}$. The evolution of the effective temperature (right scale) is also plotted. Time is in years counted from the moment at which the remnant reaches $T_{\rm eff}$ = 70 000 K. The vertical lines bracket the domain where neutrino losses exceed photon luminosity.

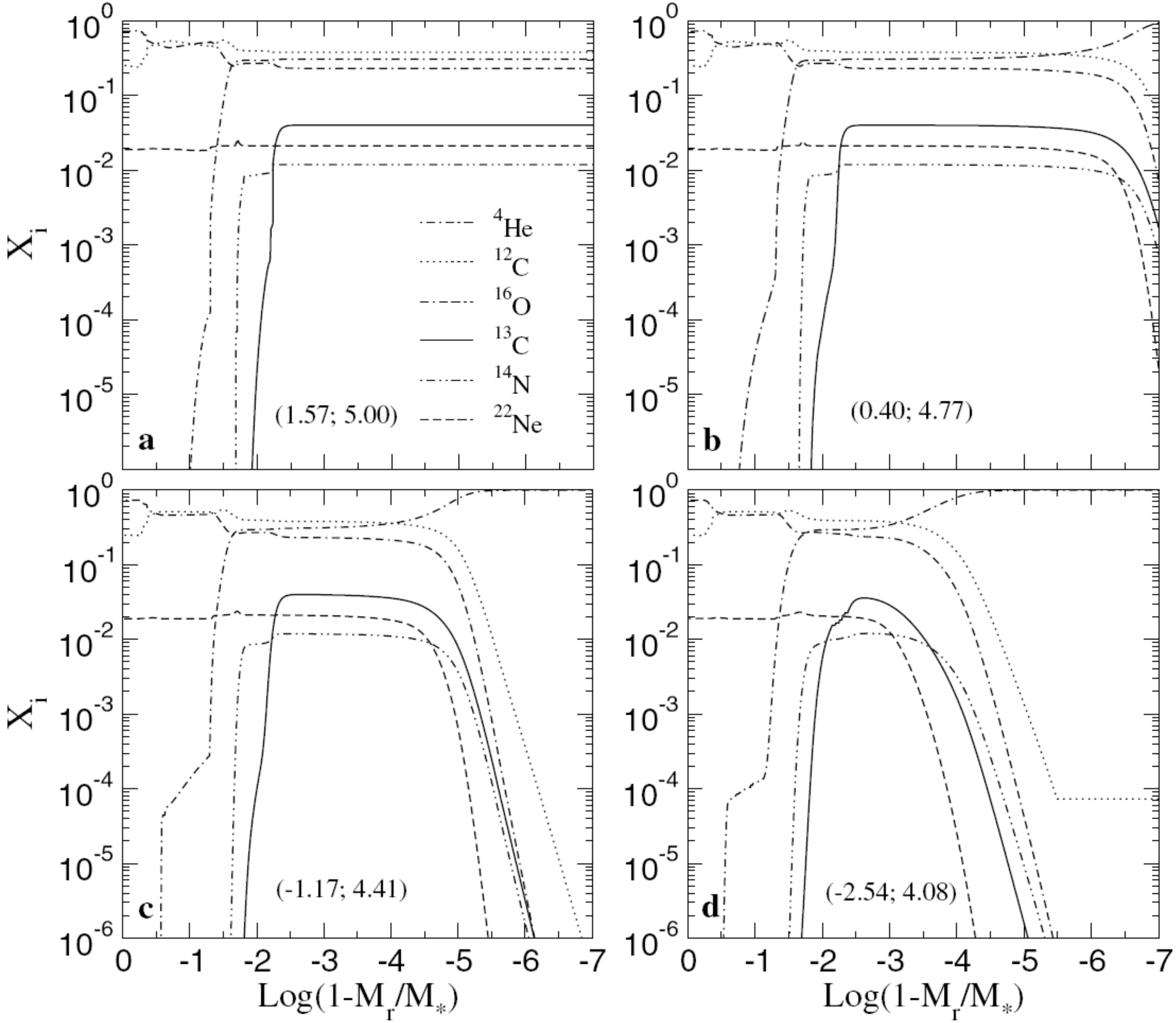

Fig. 9. Abundance by mass of ^{4}He, ^{12}C, ^{16}O, ^{13}C, ^{14}N and ^{22}Ne in terms of the outer mass fraction for the 0.5885 $M_\odot$ remnant at four selected white-dwarf evolutionary stages, characterized by values of $\log L/L_\odot$ and $\log T_{\rm eff}$ (the corresponding values are given in parentheses). Panel **a)** corresponds to the start of the cooling branch, panel **c)** to an evolutionary stage during the DB instability strip and panel **d)** to the domain of the carbon-enriched DQ white dwarfs. Panel **d)** illustrates the significant carbon enrichment in the surface layers as a result of convective dredge-up of the carbon diffusive tail by the superficial helium convection zone. It is clear that element diffusion strongly modifies the internal chemical profiles of the hydrogen-deficient white dwarf.

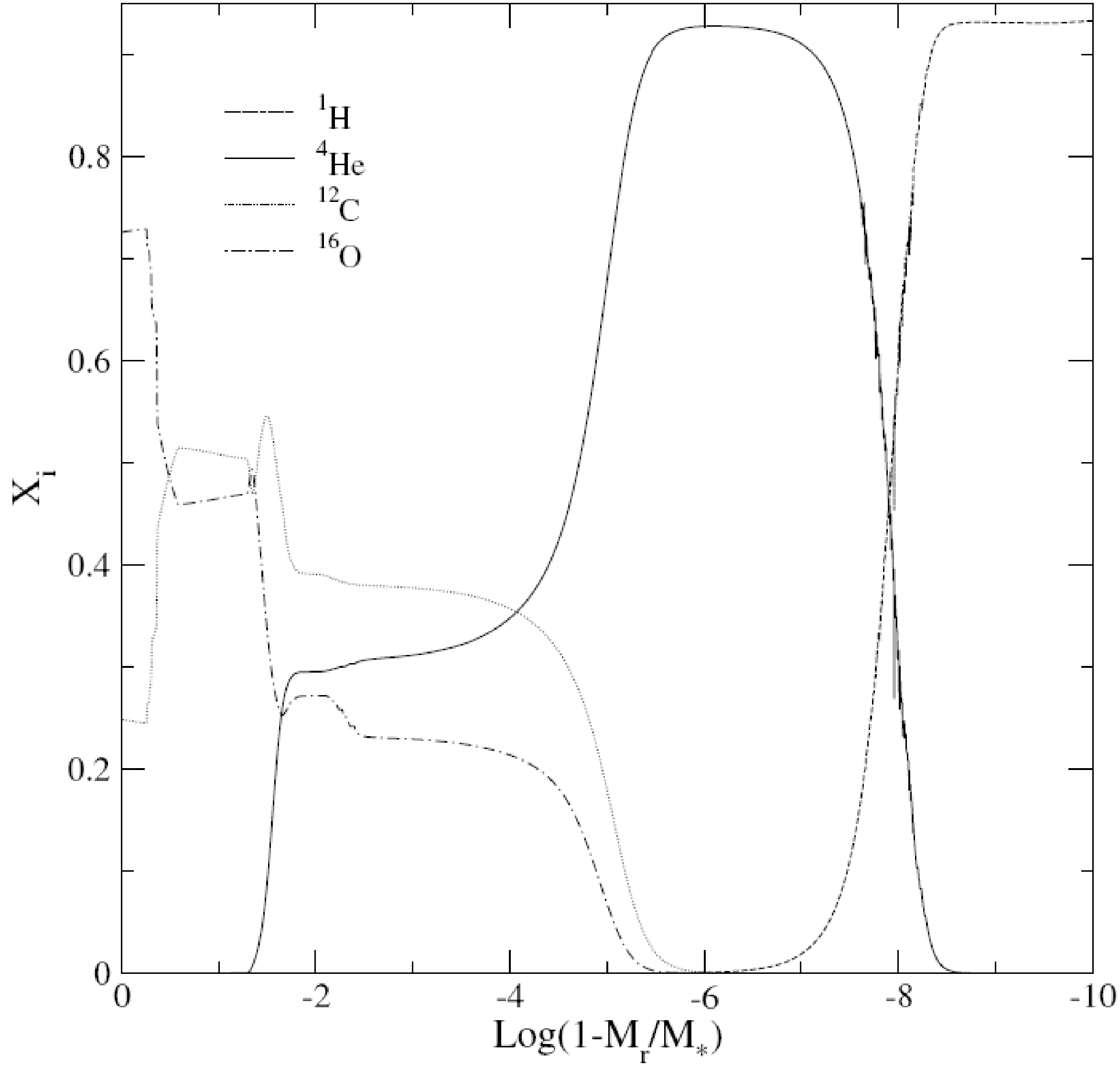

Fig. 15. Abundance by mass of ^{1}H, ^{4}He, ^{12}C and ^{16}O as a function of the outer mass fraction for the 0.5885 $M_\odot$ white dwarf remnant at $T_{\rm eff}$ = 27 000 K. Here, post-born again mass-loss episodes have been neglected. Thus, traces of hydrogen remain in the star at the beginning of white dwarf evolution. Note that element diffusion leads to the formation of a DA white dwarf with a pure hydrogen envelope mass of about 5×10^{-9} $M_\odot$. In this particular simulation, we have neglected the diffusion of minor species such as ^{13}C and ^{14}N.

DQ White Dwarfs

- $T < 13,000$K
- log(C/He) = -7.3 to -1.5
  - Due to different masses
    - Depth of convection zone
  - Or different progenitors

DQ White Dwarfs with Low C

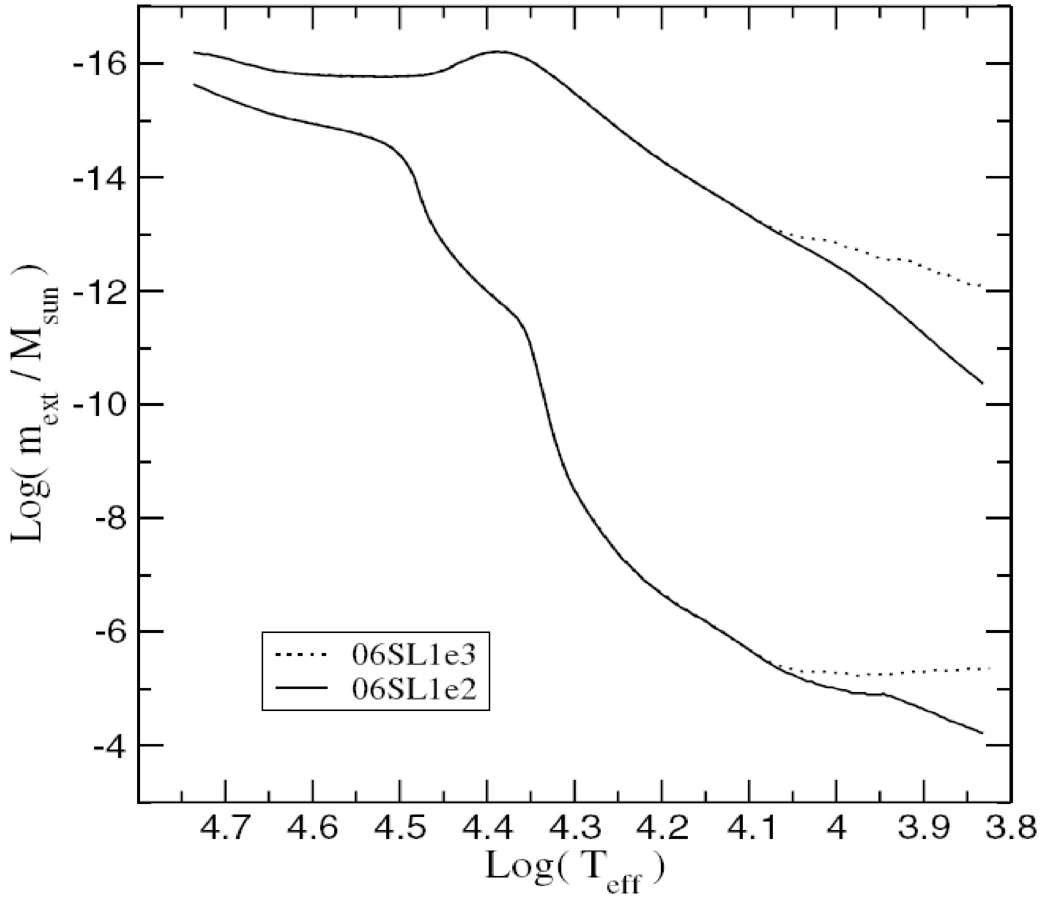

Fig. 1. *Top and bottom* layers of the OCZ expressed in terms of log ($m_{\rm ext}/M_\odot$) versus log ($T_{\rm eff}$) (being $m_{\rm ext} = M_* - M_r$) for 0.6-$M_\odot$ single-layered models with $M_{\rm He} = 10^{-2} M_*$ (solid line) and $M_{\rm He} = 10^{-3} M_*$ (dotted line). For the model with thinner helium envelope the bottom of the OCZ remains shallower from $T_{\rm eff} \sim 11\,200$ K.

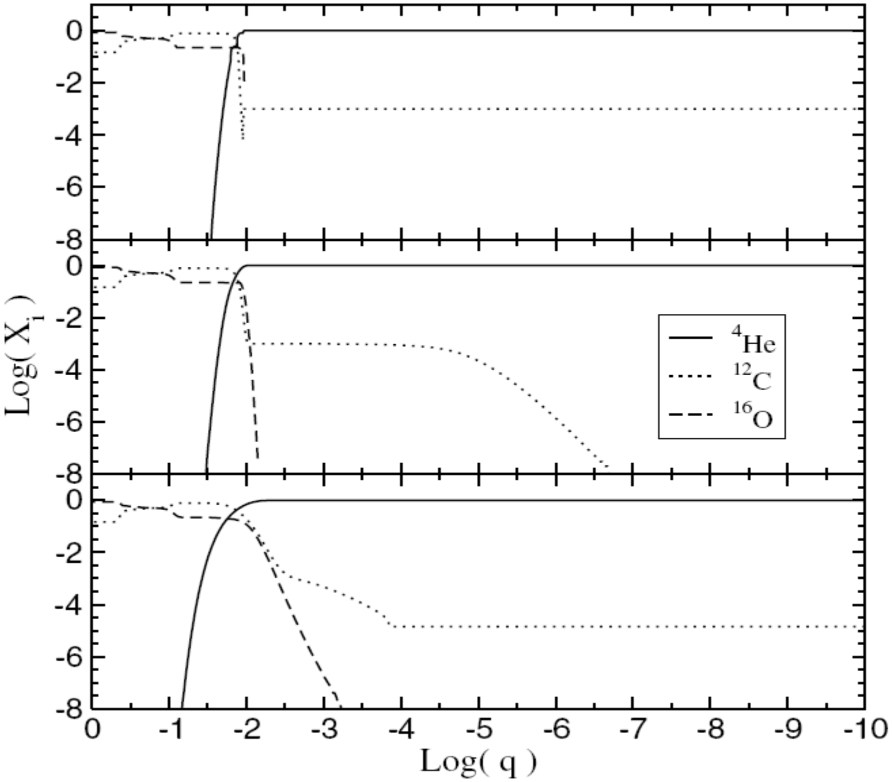

Fig. 2. Abundance (by mass) of ^{4}He, ^{12}C, and ^{16}O in terms of the outer mass fraction for 0.5-$M_\odot$ single-layered models with $M_{He} = 10^{-2}\ M_*$. The upper panel shows the situation at the beginning of the sequence. The middle panel depicts the profiles at T_{eff} = 25 700 K, and the bottom panel displays the predictions at T_{eff} = 7300 K. Note the presence of carbon in the outer layers as a result of convective dredge-up.

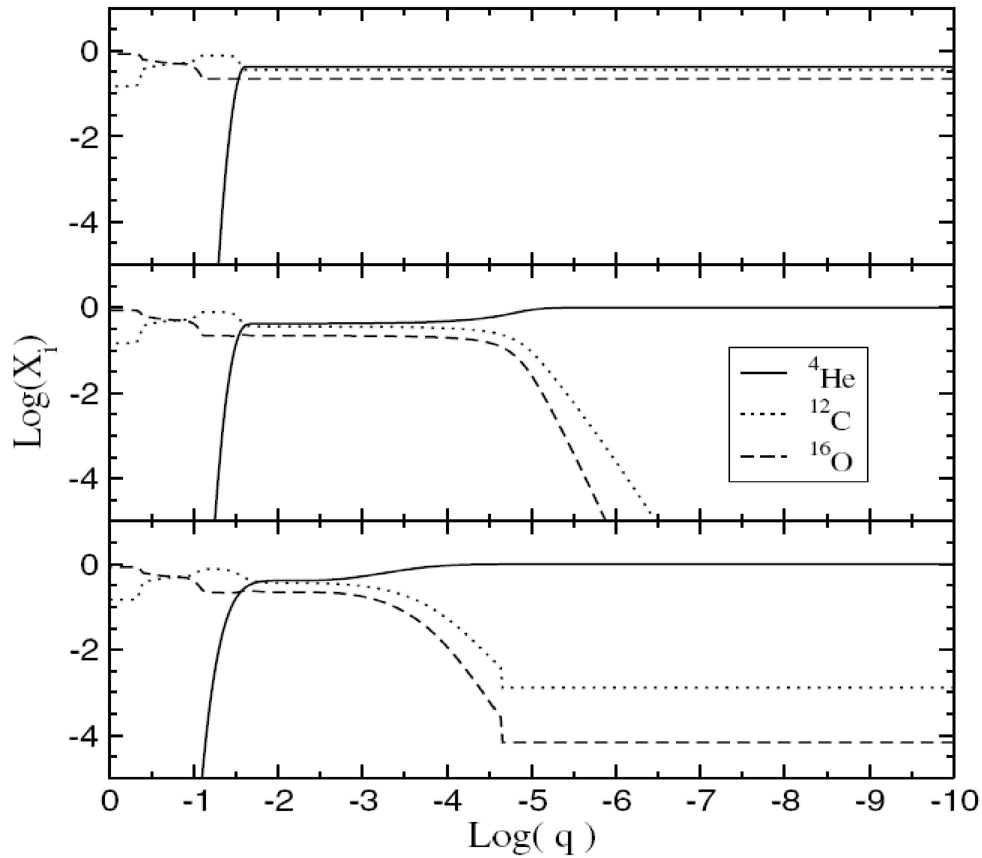

Fig. 3. Same as Fig. 2, but for double-layered models. *Upper, middle, and bottom panels* depict the situation at 49 700, 22 800, and 8900 K, respectively.

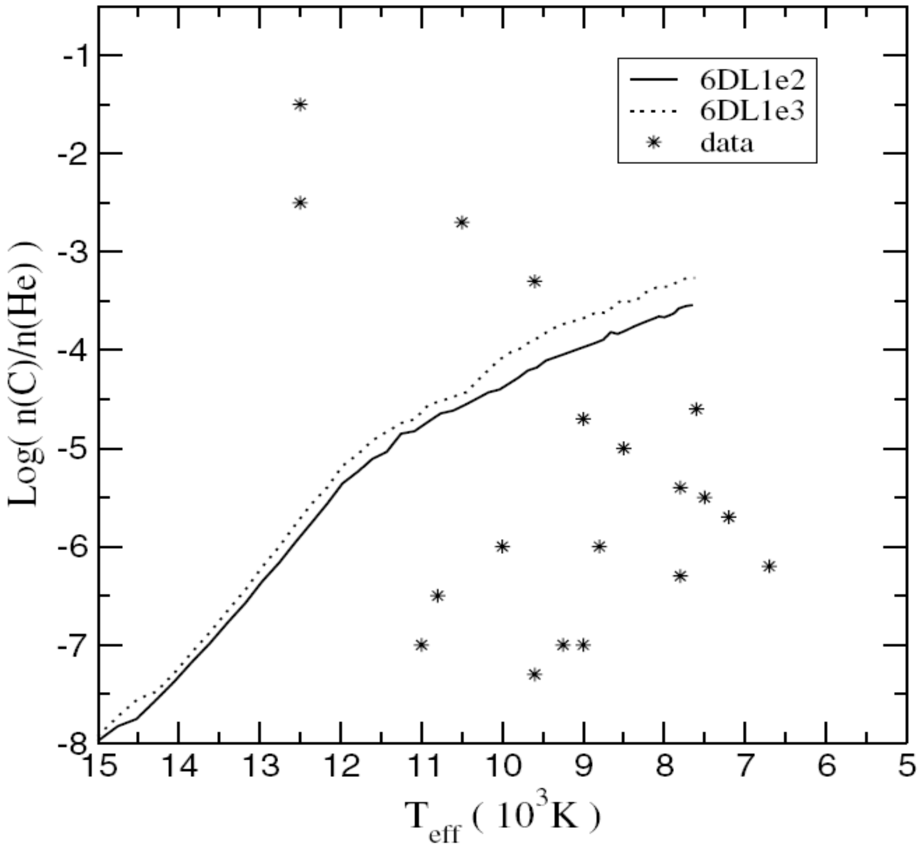

Fig. 4. Evolution of the surface carbon abundance (relative to helium abundance) for 0.6-$M_\odot$ double-layered models with $M_{He} = 10^{-3}\ M_*$ (dotted line) and $M_{He} = 10^{-2}\ M_*$ (solid line). Dots represent the observational situation as quoted by Weidemann & Koester (1995).

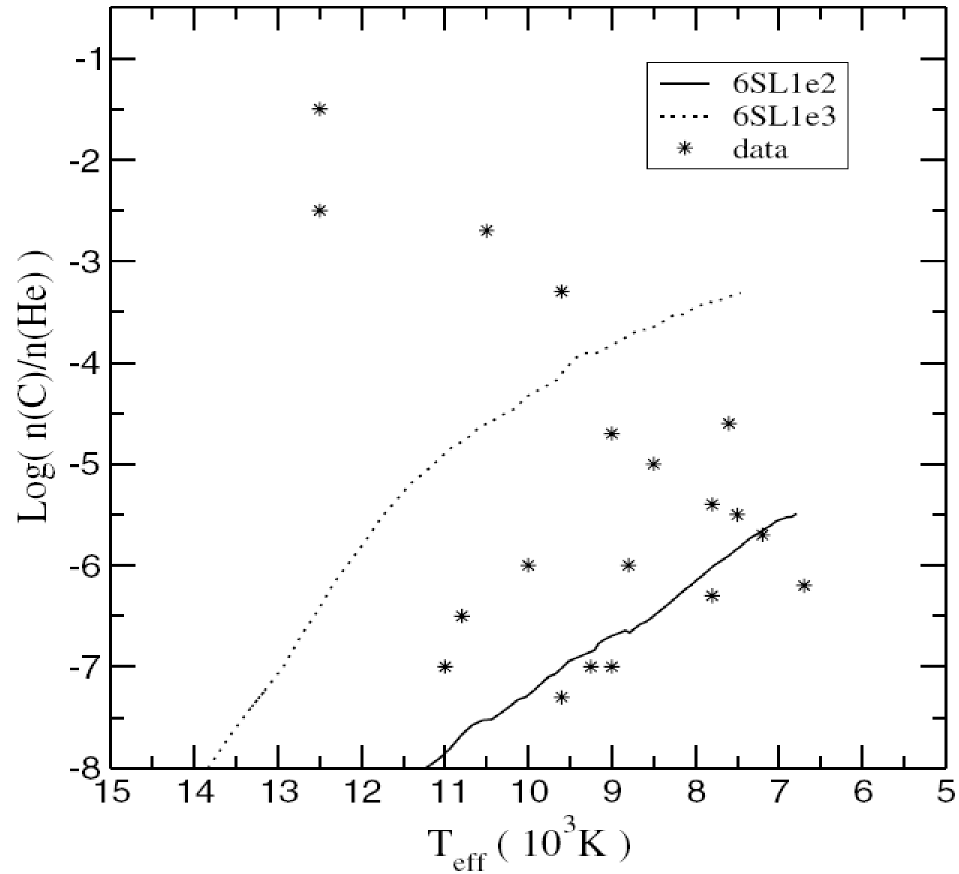

Fig. 5. Same as Fig. 4 but for single-layered models. Remarkably, thin envelope models exhibit a rather large carbon abundance as compared with the case of thick envelope models. See text for additional details.

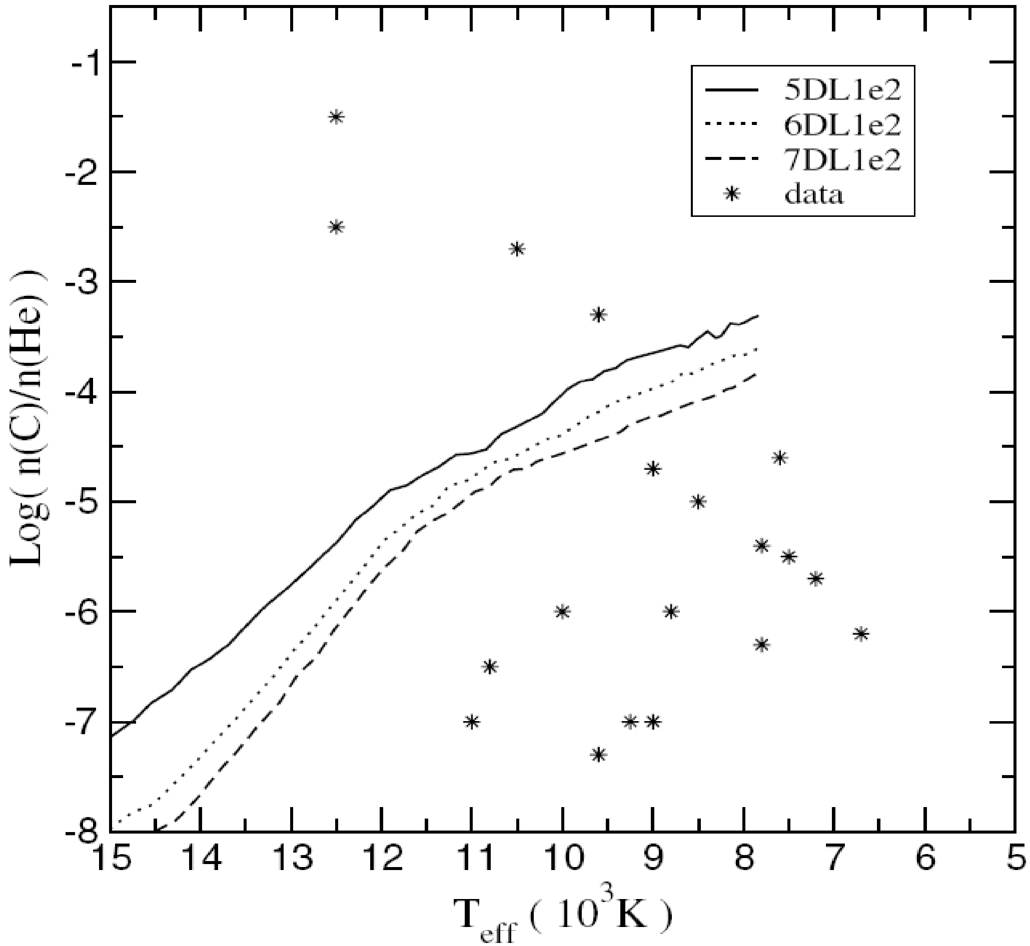

Fig. 6. Same as Fig. 4 but for double-layered models with different stellar masses and equal helium content.

DO White Dwarfs

- 45,000K < T < 120,000K
- Possibly originate as PG 1159 stars

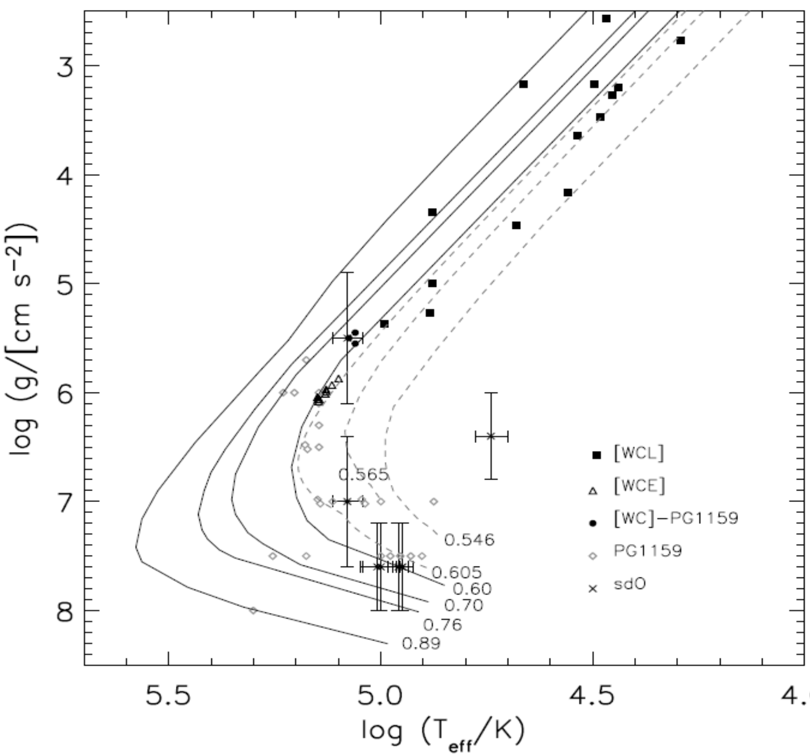

Fig. 3. Positions of the new PG 1159 stars (with error bars) compared to evolutionary tracks from Blöcker (1995), Schönberner (1983) (dashed lines) and Wood & Faulkner (1986). Labels: mass in $M_\odot$.

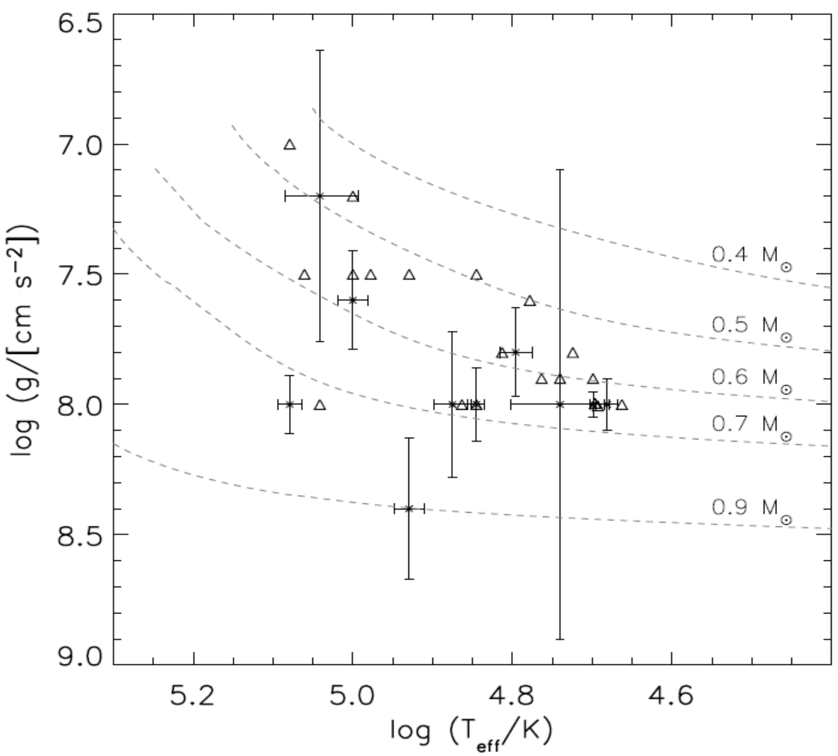

Fig. 4. Positions of DO white dwarfs compared with evolutionary tracks from Wood (1995). The triangles represent the 19 hitherto known DOs (see Dreizler & Werner 1996; Dreizler et al. 1997; Werner et al. 2004).

DC White Dwarfs

- $T < 11{,}000K$
  - Old
  - Not “white” anymore
- May have H or He dominated atmosphere
- Spectrum may be effected by collision-induced absorption
  - Collisions between H_2 and H, He atoms and molecules induces temporary dipole (discussed last week)

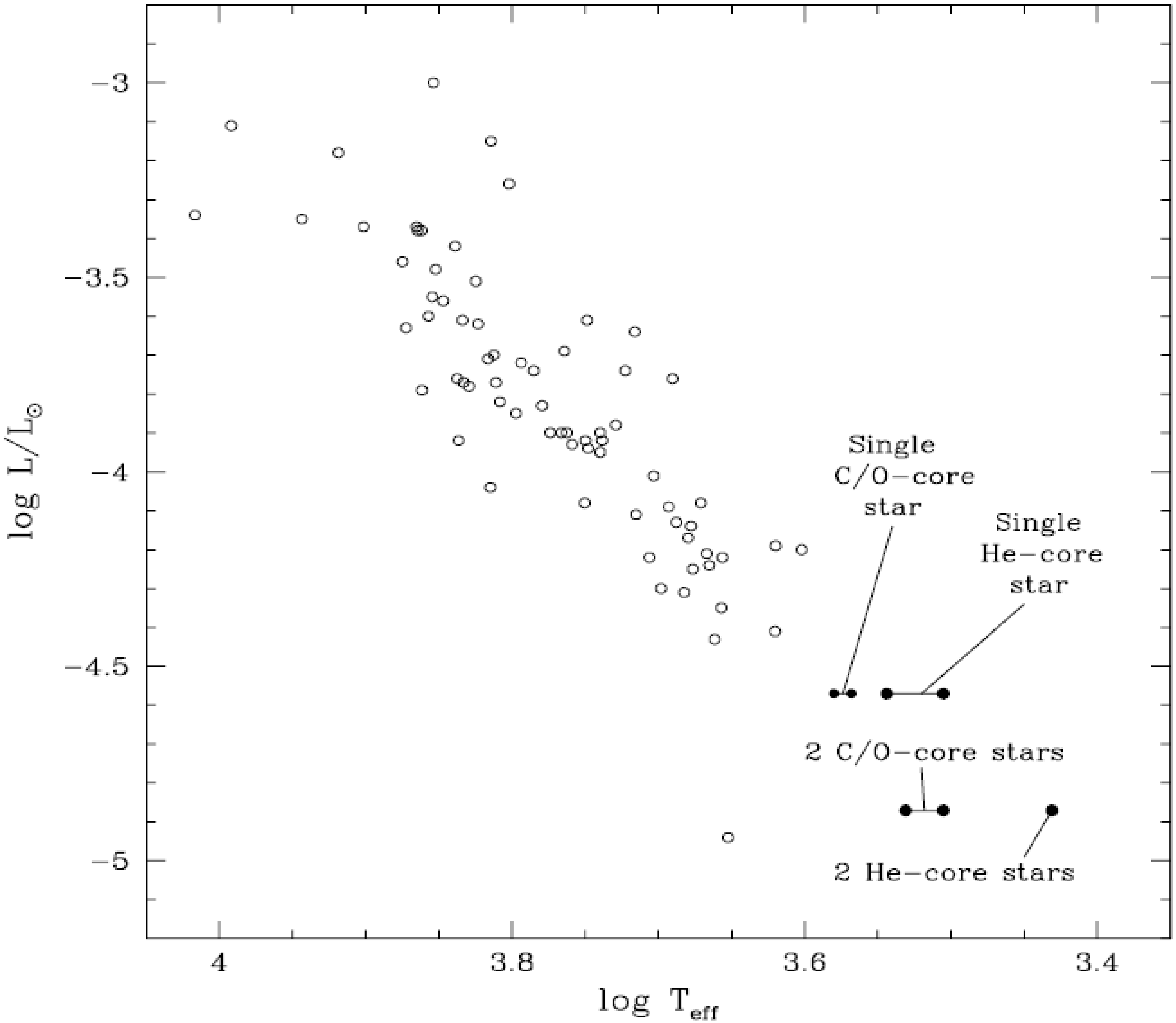

FIG. 6.—H-R diagram showing LHS 3250 with a sample of cool white dwarfs. LHS 3250 is plotted with two filled circles to show a plausible range of (cool) temperatures.

DZ White Dwarfs

- T probably < 11,000K
- C, Ca, Mg, Fe, Si in a generally He atmosphere
- Accretion from ISM
  - Passage through dense interstellar cloud
  - H/metal ratio much lower than in Sun
    - Somehow H is not accreted

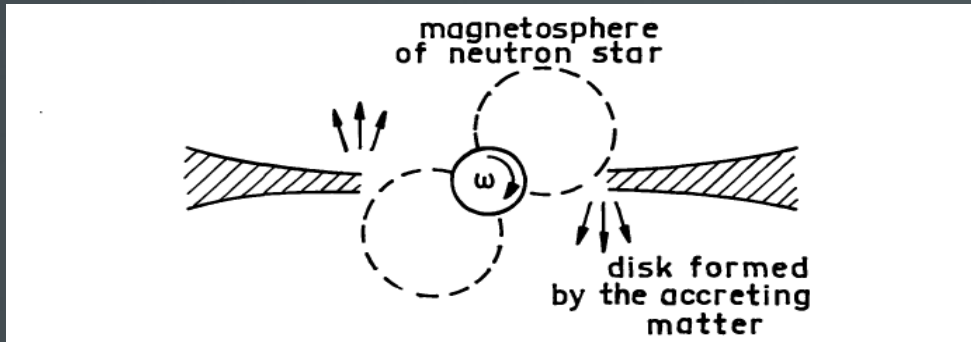

Fig. 3. Schematic picture, illustrating the interaction of "propeller" with accreting disk. Rotating magnetosphere destroys the disk and throws away the accreting matter from the neutron star

Illarionov and Sunyaev 1975, A&A, 39, 185

Summary